Simulations of vertical ion-drag effect on neutral winds and density at low and middle latitudes

EQIT-07

Qingyu Zhu[1] (Qingyu.zhu@mavs.uta.edu), Yue Deng[1], Astrid Maute[2], Arthur D. Richmond[2]

1. University of Texas, Arlington 2. HAO, NCAR, Boulder

ABSTRACT

The effects of vertical ion-drag force on the vertical winds in the equatorial region may contribute to the generation of the crests of the equatorial thermosphere anomaly (ETA). However, such effect has not been well studied by most general circulation models (GCMs) currently due to the hydrostatic assumption carried by most GCMs. The non-hydrostatic global ionosphere and thermosphere model (GITM) solves the vertical momentum equation and thus offers the opportunity to evaluate the relative contribution of ion-drag force to the vertical momentum change of vertical winds and density in the low latitudes. In this study, GITM simulations have been conducted by coupling with the newly developed 3D ionospheric electrodynamo model to improve the electrodynamics of GITM at low latitudes. The variations of vertical winds, neutral density after introducing the electrodynamics have been examined. Furthermore, the vertical ion-drag effect on neutral winds and density at low and middle latitudes has been investigated qualitatively and compared with the impact of horizontal ion-drag force.

MOTIVATIONS

1. Daytime eastward electric field → predominant upward ion drift at equatorial region→ EIA;
2. Observations show the coupling between EIA and ETA [e.g. Liu et al. 2007, Lei et al. 2010];
3. The impact of the vertical ion-drag force on vertical neutral winds and neutral density may contribute to the formation of ETA;

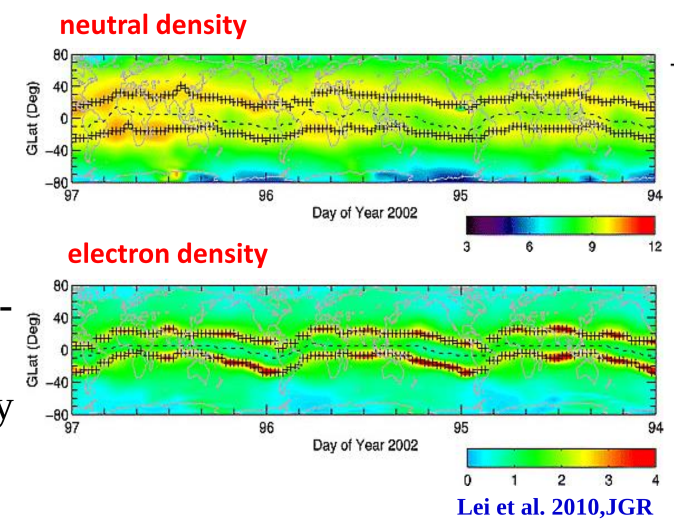

Vertical momentum equation:

$$\frac{\partial U_z}{\partial t} + \vec{U}\cdot\nabla U_z = -\frac{1}{\rho}\frac{\partial p}{\partial z} + \vec{g} + \vec{F_z} \quad (1)$$

$-\frac{1}{\rho}\frac{\partial p}{\partial z} + \vec{g}$ represents the **buoyancy term** and **vanishes when reaching hydrostatic equilibrium**

$\vec{F_z}$ represents the **vertical ion-drag force**

Highlights of GITM

- Flexible grid resolution
- Solves in altitude coordinates
- **Non-hydrostatic solutions**

Highlights of 3D electrodynamo model

- Fixed height grids (correspond to the apex heights of field lines at low latitudes)
- Using a staggered grid
- Self-consistent calculation of 3D current system
- Using 3D apex quantities (Richmond 1995)

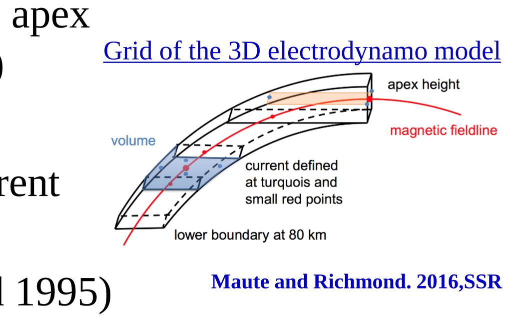

Electric fields: $\vec{E} = E_{d1}\vec{d_1} + E_{d2}\vec{d_2}$ (2)

- **Geomagnetic eastward** electric field
- Ed1 is **constant** along the magnetic field line

1. METHODOLOGY

mLat-mLon distribution of Ed1 in APEX frame 1200 UT

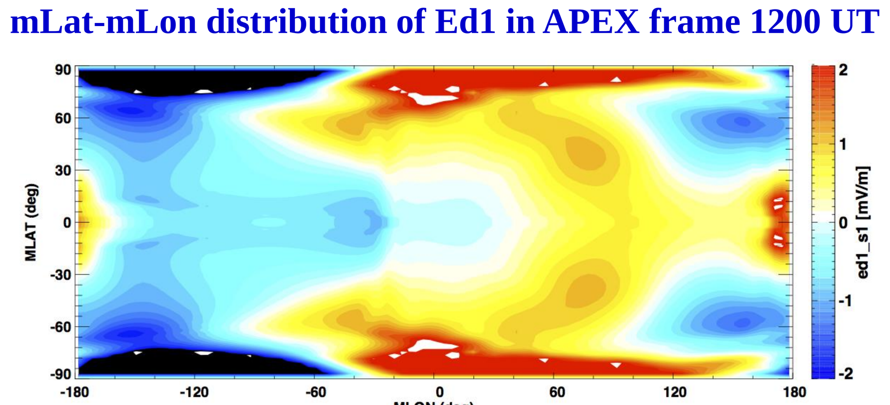

Simulations in 3D electrodynamo model

- Obtain the distribution of Ed1 from 3D electrodynamo model with the input of winds and conductivities from TIEGCM.
- Solar maximum; quiet time; equinox

(a) Lat-Lon distribution of eastward electric field 1205UT

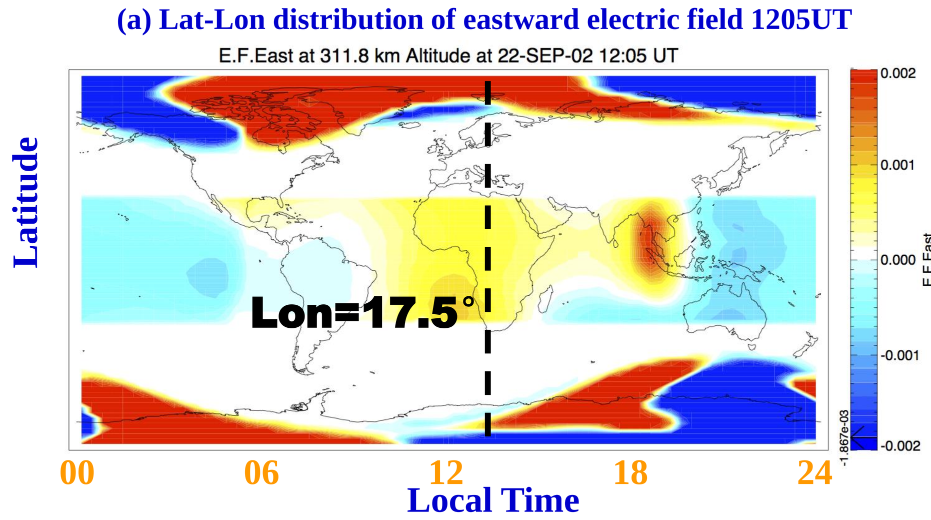

(b) Lat-Lon distribution of vertical ExB 1205UT

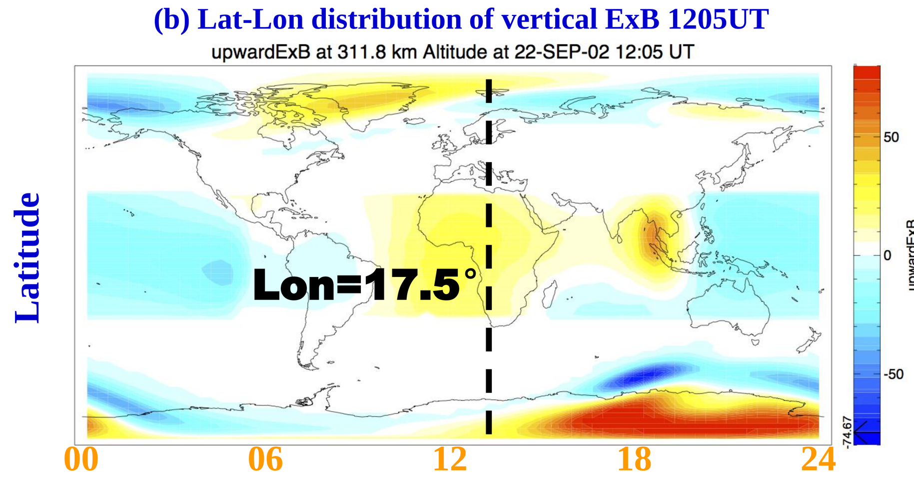

Simulations in GITM:

- Resolution: 5° Lon x 2.5° Lat
- The Ed1 from 3D electrodynamo model has been interpolated into GITM , but only the electric fields within the geographic latitudes of ±30° are kept. The high-latitude electric fields come from the Weimer's model.
- Simulation time interval: 1200-1300UT
- September equinox, quiet geomagnetic condition
- Two simulations have been conducted, with/without the imposed electric fields within the geographic latitudes of ±30°. The differences between these two simulations have been displayed in the coming figures (**geographic coordinate**). The Longitude of 17.5° has been studied. (geomagnetic equator is at 11° N)

2. VERTICAL WINDS AND BUOYANCY

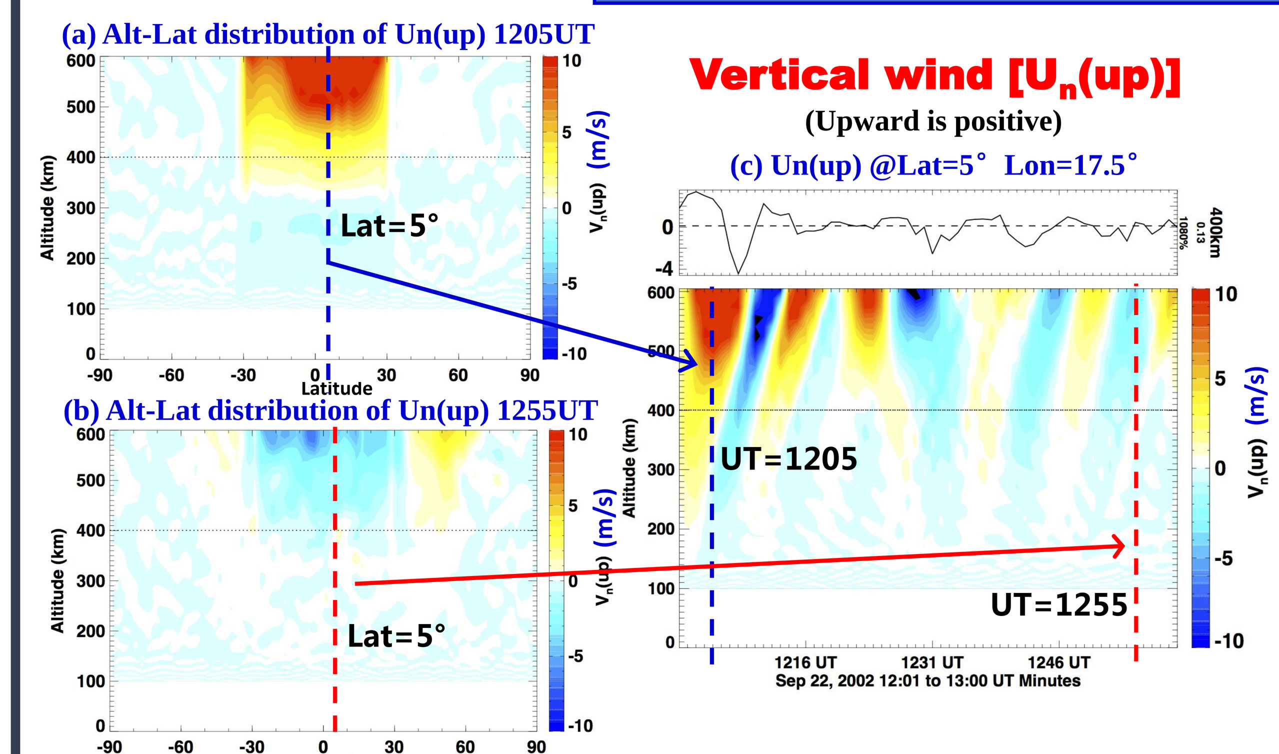

- (a), (b): alt-lat distribution of Un(up) at 1205 UT and 1255UT ; (c): the temporal variation of Un(up) at Lat=5°
- Figs a and b show that the Un(up) significantly changes near the magnetic equator. The magnitude can reach **10 m/s** over 500 km at the beginning
- Fig c displays that the **wave structures** show up in Un after the inclusion of electric fields. The magnitude of the primary oscillations can reach **4 m/s** at the altitude of 400 km

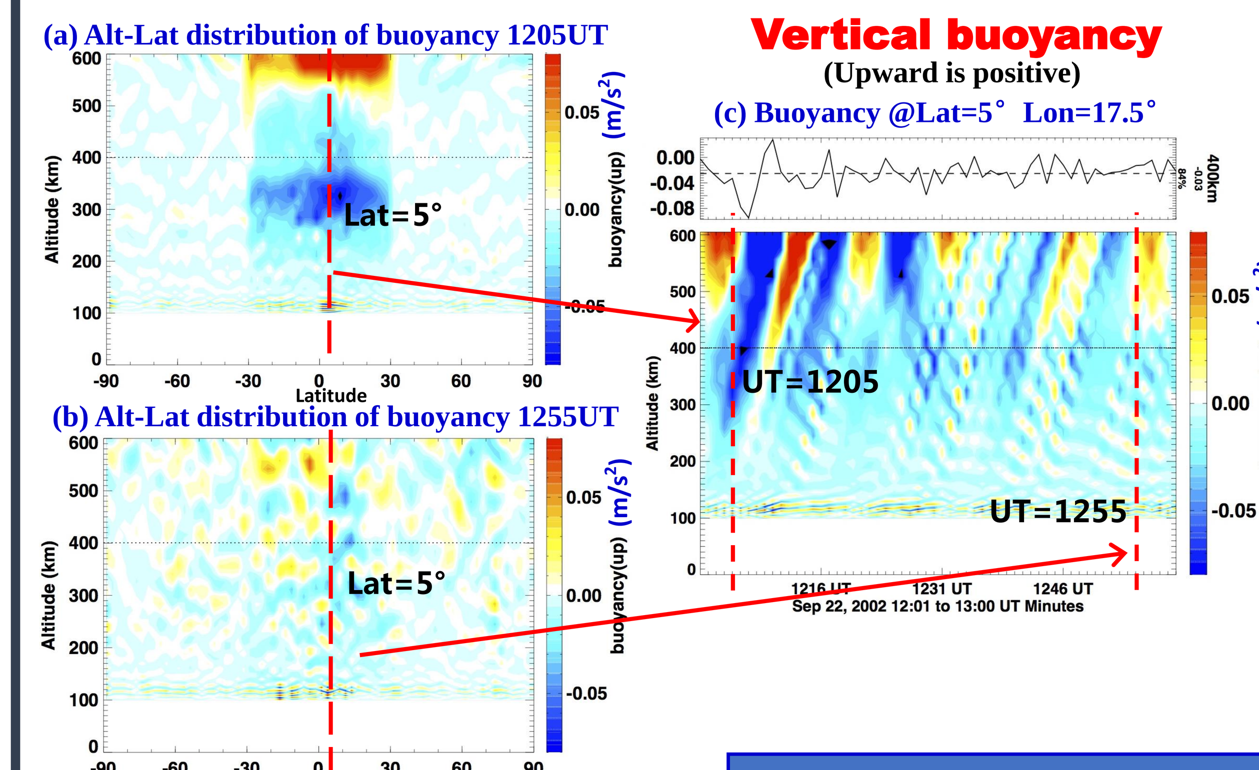

- Same format as vertical Un but for buoyancy $-\frac{1}{\rho}\frac{\partial p}{\partial z} + \vec{g}$.
- Figs a and b show that the significant changes of buoyancy take place near the dip equator at the beginning and becomes more indistinct when reaching the end.
- Fig c shows that **wave structures** are also apparent in the buoyancy term; the primary oscillation can reach **-0.1 m/s²** at 400 km , suggesting that the gravity and pressure gradient force are out of balance by **1-2%.**

4. VERTICAL ION-DRAG FORCE AND MERIDIONAL ION-DRAG FORCE

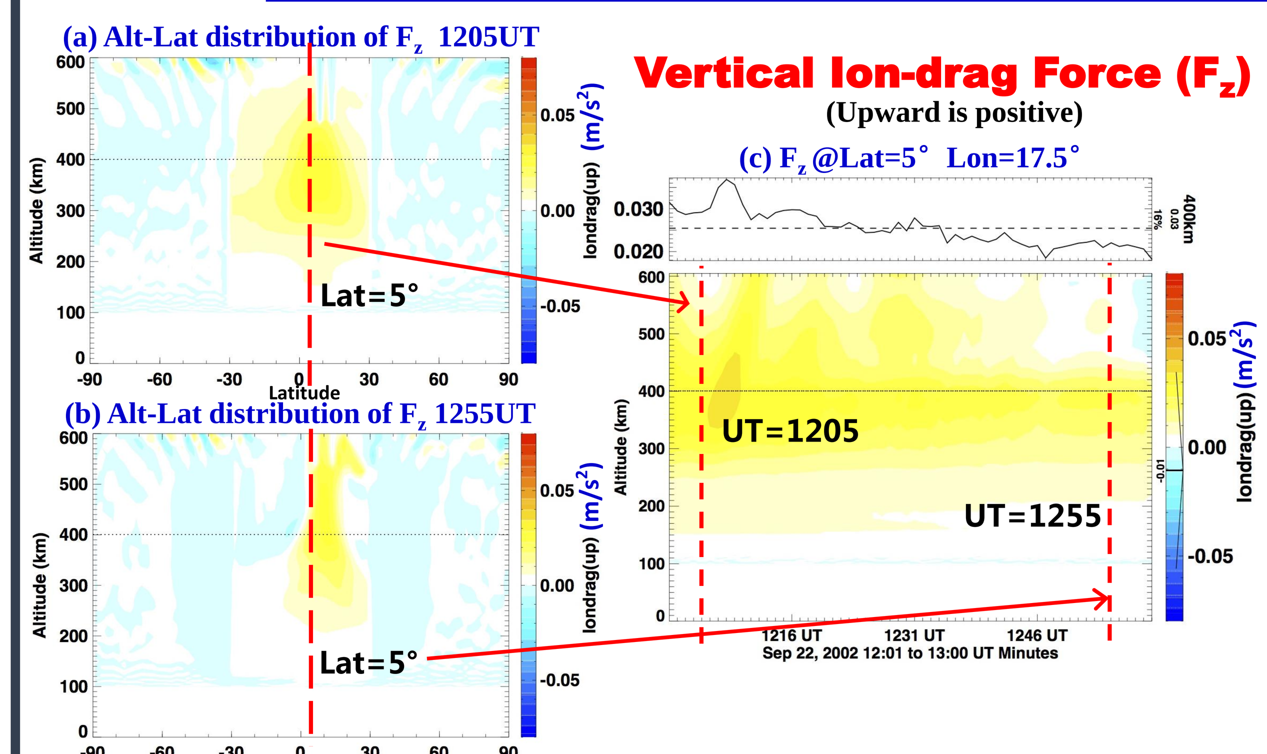

- Fig a shows that the change of vertical ion-drag force is apparent near the dip equator just after the inclusion of electric field and it can reach **0.03 m/s²** at 400 km
- Fig b shows that the latitudinal range of large ion drag force becomes **narrower** at the end.
- Fig c shows that the ion drag force at Lat = 5° experience a reduction as the time increases above 400 km

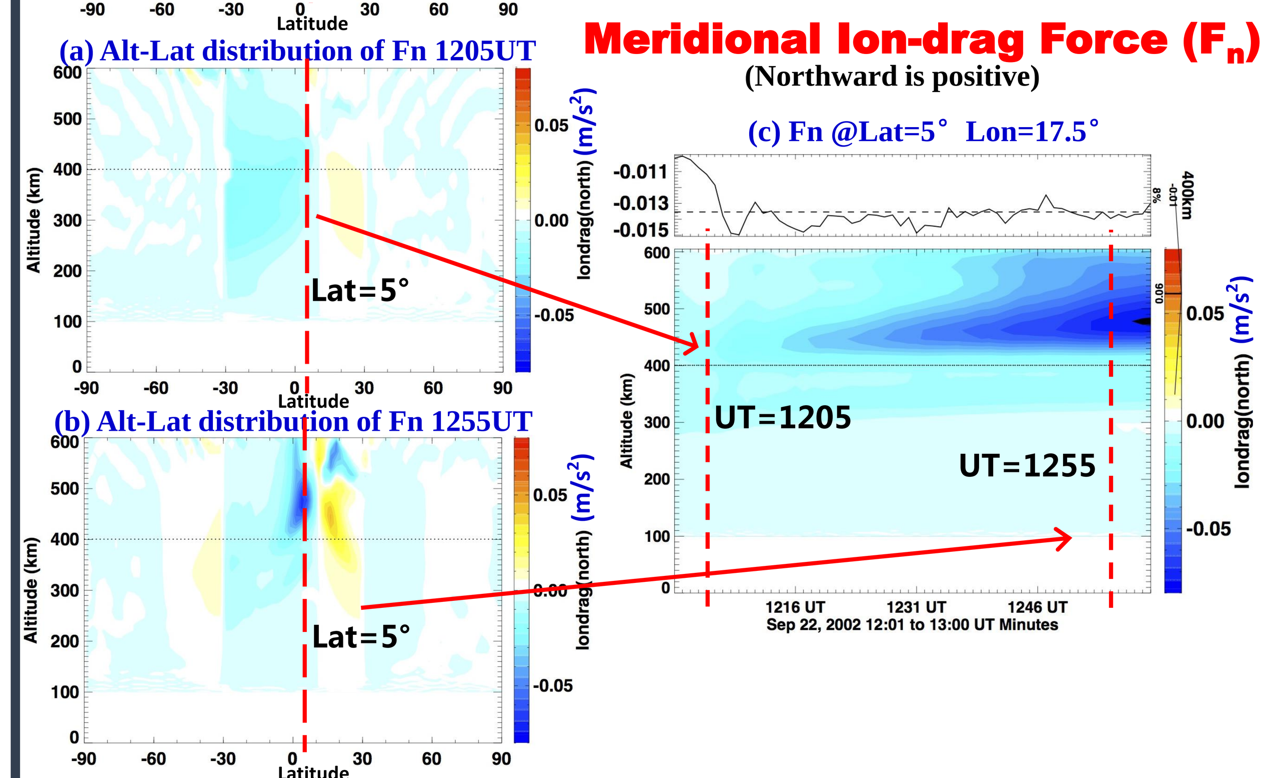

- Fig a shows that the poleward ion-drag force exists at the beginning (**-0.02 ~0.01m/s²** at 400 km).
- Fig b exhibits that when reaching the end of the simulation, the meridional ion-drag force becomes more preeminent (**-0.03~0.03 m/s²** at 400 km).
- As compared with vertical ion-drag force, **meridional ion-drag force is weaker than vertical ion-drag force at the beginning and then becomes dominant** (>400 km) **after 15-20 min.**
- **Vertical ion-drag force can push the neutral density to high altitudes near the dip equator and then the poleward ion-drag force transfers the neutral density away from the dip equator, which may contribute to the formation of the trough and crests of ETA.**

3. ELECTRON DENSITY AND NEUTRAL DENSITY

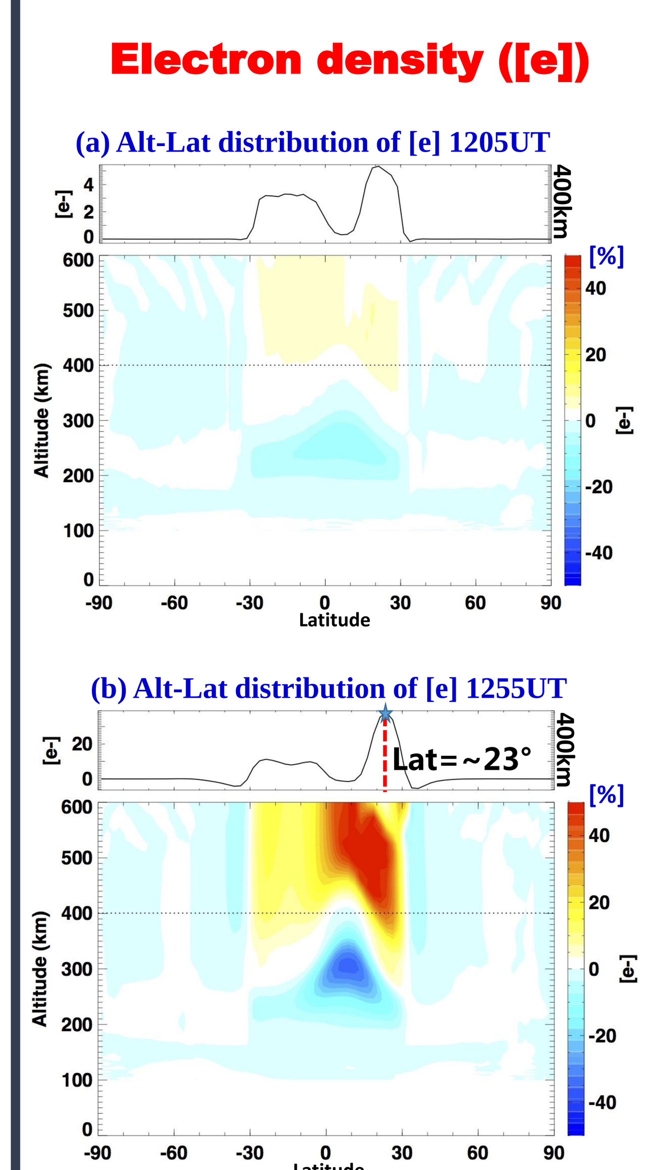

- The EIA crests and trough show up right after the inclusion of electric fields and become more pronounced as the time increases.
- The northern crest is well formed at geographic latitude of **23°** (**12°** away from the dip equator) while the southern crest is more spread and weaker than the northern one.

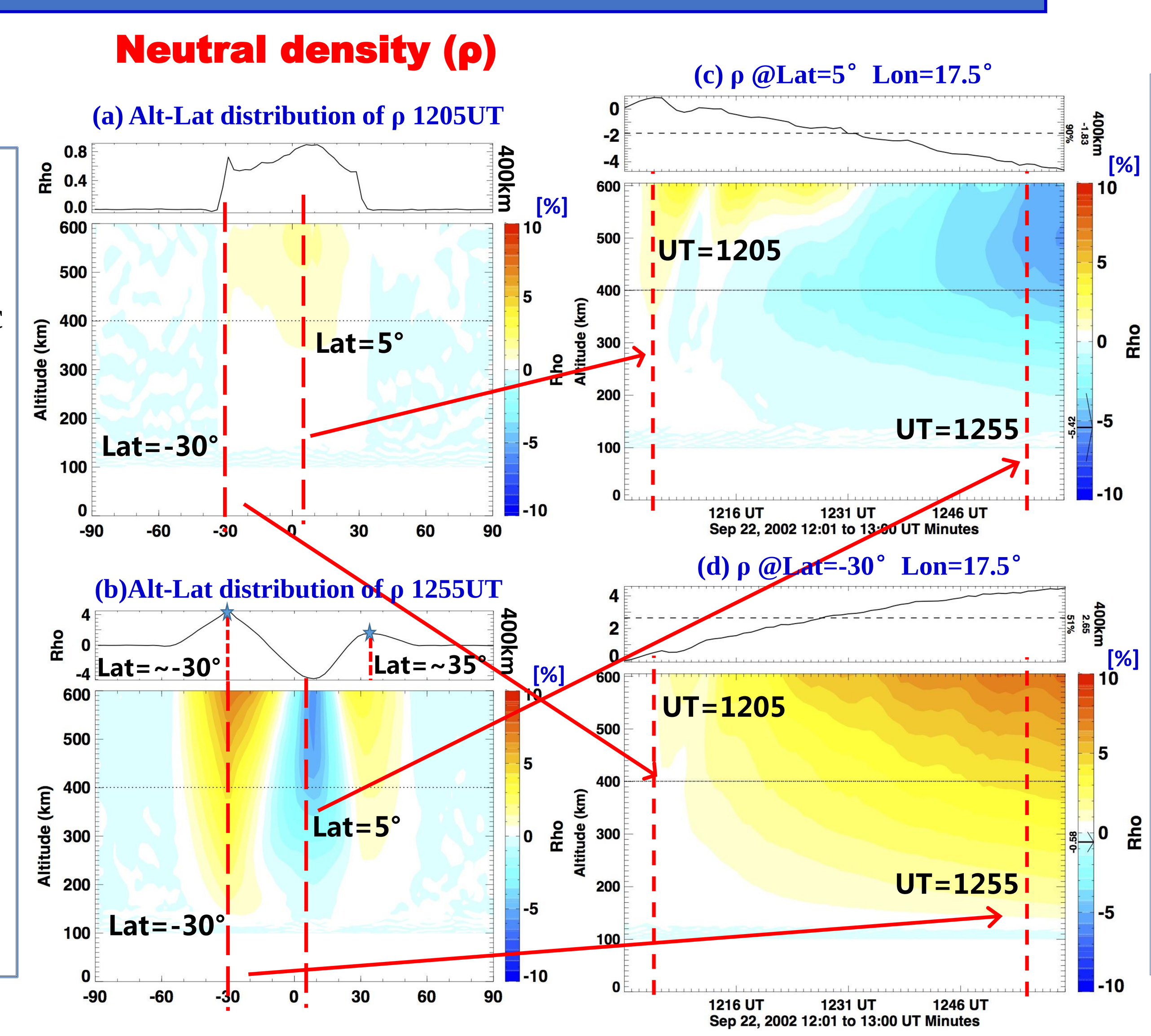

- Fig a shows that the neutral density near the dip equator increases **~1-2%** at the top at the beginning
- At 1255UT (Fig b) the **trough** of neutral density shows up near the **dip equator** and the **crests** appear at Geo Lat= **~ -30° and 35°** at 400 km respectively (**~40° , 25°** away from dip equator)
- **Enhancement** at the **crest =4%**; **Depletion** at the trough = **-4%**; **→ crest/trough =1.08** (close to CHAMP's observation)
- Figs c and d show that the density at the dip equator decreases after the initial enhancement while the density near the crest increases continuously.

5. CONCLUSION

- The vertical ion drift imposes vertical ion-drag force of 0.03 m/s² on the vertical neutral winds at the beginning and influences the motion of vertical wind near the dip equator. The pressure gradient force and gravity are out of balance by 1-2% due to the vertical ion-drag force.
- Both of neutral density and electron density show trough and crests after the inclusion of the eastward electric field. Their troughs correspond to the magnetic equator well. The crests of neutral density is ~25-40° away from the magnetic equator and are more poleward than the crests of electron density.
- Vertical ion-drag force pushes the neutral density to high altitudes near the magnetic equator and subsides to the meridional ion-drag force as the time increase. The poleward ion-drag force transfers the neutral density away from the magnetic equator, which may contribute to the formation of the trough and crests of ETA.